ORIGINAL ARTICLE

Assessing sediment yield and sources using fingerprinting method in a representative catchment of the Loess Plateau, China

Peng Tian[1] · Zhengfeng An[2] · Guangju Zhao[2,3] · Peng Gao[2,3] · Pengfei Li[2,3] · Wenyi Sun[2,3] · Xingmin Mu[2,3]

Abstract

Quantitative assessment of sediment yield and sources is of great importance for future soil and water conservation and watershed management in erosion-prone areas. This study investigated sediment yield and sources by using a simple fingerprinting method in a dam-controlled watershed on the northern Loess Plateau. The sampling sediment profile exhibited 24 flood couplets corresponding to rainfall storms from 2001 to 2014. A total of 2.05×10^5 t sediment was trapped during the period. The annual sediment yield varied from 0 to 430 t ha^{-1} year^{-1}, with an average annual sediment yield of 146.1 t ha^{-1} year^{-1}. Ten sediment properties (i.e., σ^{13}C, σ^{15}N, TOC, TN, C/N, X_{lf}, X_{hf}, X_{fd}, ^{137}Cs, ^{210}Pb) were potentially selected to identify the sediment sources. The multivariate discriminant function analysis (DFA) test suggested that three soil properties (X_{hf}, TN, and ^{137}Cs) comprised the optimum composite fingerprinting. The results demonstrated that sandstone contributed nearly 90% of sediment in 2012 and 56.1% in 2003. The contribution from arable land varied from 5.2% in 2005 to 44.6% within the period of 2013–2014. On average, approximately 74.06% of sediment originated from the weathered sandstone, followed by 15.67% from arable land, and the remaining 10.27% from uncultivated land. Our finding indicated that bare sandstone was the main sediment source, leading to relatively high sediment yield in the study area. This study provides a method with great potential for sediment yields assessment and sediment source identification in ungauged watersheds on the Loess Plateau.

Keywords Check dam · Fingerprinting method · Sediment yield · Sediment sources · Loess Plateau

Introduction

Soil erosion has been widely recognized as one of the most important forms of land degradation across the world and is greatly influenced by land use/cover, soil types, climate, and lithology (Fleskens and Stringer 2014). The Chinese Loess Plateau has been ranked as one of the most severely eroded areas in the world (Hessel 2006; Jiao et al. 2014). Severe soil erosion leads to loss of surface soil resulting in the degradation of soil quality and reduction of agricultural production, threatening food and environmental security at a regional scale (de Vente et al. 2006; Mukundan et al. 2010). Besides, the siltation of reservoirs and riverbeds has become a critical off-site problem resulting from high soil erosion rates and sediment delivery ratios in the Yellow River basin (Wang and Jiao 1996). This is particularly important for those areas in the middle and lower reaches, where many reservoirs were rapidly silted. It is necessary to assess present and historical soil erosion rates and sediment sources for the continued improvement of soil conservation practices (Foster and Walling 1994; Fox and Papanicolaou 2007).

Direct continuous field measurements with sufficient spatial coverage are very useful to understand sediment yield and its variation across a watershed. However, long-term field monitoring is time consuming, costly, and sediment yields are difficult to obtain because of the trapping effect of check dams and conservation measures on hillslopes. In this context, many researchers derived sediment yields through sedimentation in deposit facilities such as reservoirs and check dams (Bussi et al. 2013; de Vente et al. 2006;

✉ Xingmin Mu
  xmmiswc@gmail.com

1 College of Natural Resources and Environment, Northwest A&F University, 26 Xinong Road, Yangling 712100, Shaanxi Province, China

2 State Key Laboratory of Soil Erosion and Dryland Farming on the Loess Plateau, Northwest A&F University, 26 Xinong Road, Yangling 712100, Shaanxi Province, China

3 Institute of Soil and Water Conservation, Chinese Academy of Sciences & Ministry of Water Resources, 26 Xinong Road, Yangling 712100, Shaanxi Province, China

Grauso et al. 2008; Mekonnen et al. 2015; Palazón et al. 2016; Romero-Díaz et al. 2007; Van Rompaey et al. 2007; Verstraeten and Prosser 2008; Zhang et al. 2004, 2017). On the Loess Plateau, check dams have become one of the key soil conservation and sediment control measures (Zhao et al. 2017a). Thus far, more than 110,000 sizable check dams have been built (Xu et al. 2004; Zhang et al. 2009; Zhao et al. 2017b). Such check dams offered an opportunity to reconstruct the records of annual and event-based sediment yields for small catchments (Jin et al. 2012), which provides a useful reference for understanding historical changes of sediment yield in a specific region (Zhang et al. 2017; Zhao et al. 2017b, c).

The fingerprinting method, known as the sediment source apportionment procedure, has been increasingly applied to identify relative contributions of the corresponding sediment sources (Collins et al. 2010; Navas et al. 2014; Pulley and Rowntree 2016; Walling et al. 2008; Wilkinson et al. 2013; Zhang and Liu 2016; Zhang et al. 2016). Different soil properties have been used as fingerprints to identify the sediment sources, including soil physical, geochemical, isotopical, and biological properties (Collins et al. 1997; Walling 2005; Zhang and Liu 2016). Tracer selection plays a critical role in sediment source fingerprinting, since different tracers may yield different proportional contributions (Laceby et al. 2017). As Zhang and Liu (2016) addressed, the nonparametric Kruskal–Wallis H test or Mann–Whitney U test can be used for tracer selection, and then a bracket test is used to remove non-conservative tracers (Collins et al. 2010; Mukundan et al. 2010), and the discriminant function analysis or other multivariate variance analysis is finally applied to reduce the tracer number and to identify an optimum set of tracers (Collins et al. 1997, 2010; Davis and Fox 2009; Franz et al. 2014; Guzmán et al. 2013). Afterwards, the linear mixing model is used to quantify the relative contributions from different sediment sources (Collins et al. 2010; Zhang and Liu 2016; Zhao et al. 2017c).

More recently, much attention has been paid to uncertainty assessment of the estimated source contributions. Numerical methods such as Monte Carlo simulation and Bayesian uncertainty framework have been used to simulate probability distribution of estimated source proportions (Koiter et al. 2013; Laceby and Olley 2014). Overall, significant progress has been made to advance the fingerprint technique in the past decades. The tracer-based fingerprinting methods can be used to enhance the knowledge of soil erosion processes and improve understanding of soil erosion patterns and sediment yields, particularly for the Loess Plateau with significant changes in land surface. The fingerprinting approach can provide more useful information on sediment yield and sources in the watershed, in which the hydrological processes have been altered by dams, terraces, and other conservation measures. Thus, the objectives of

this paper are (1) to explore the historical soil erosion rates through dam's sedimentation and (2) to quantify the relative contribution of the potential sources using a sediment fingerprinting technique in the northern Loess Plateau.
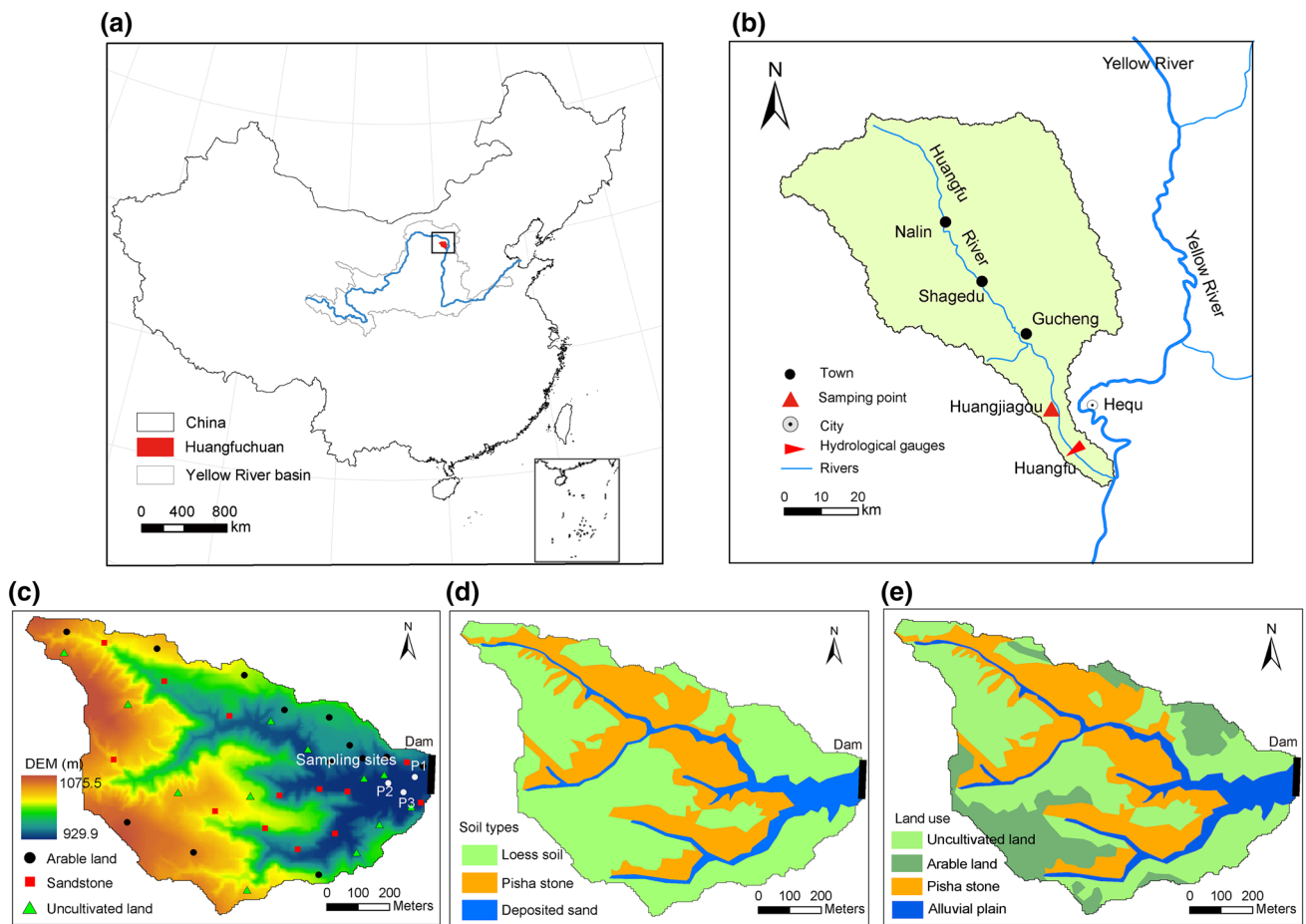
Study area

The study was conducted in the Huangjiagou watershed, a small watershed with a drainage area of 1.04 km^2 in the lower reaches of the Huangfuchuan watershed in the northern Shaanxi Province (Fig. 1). The watershed belongs to the wind-water erosion crisis region, which is characterized by a semiarid continental climate with average annual rainfall of 350–450 mm and an average annual pan evaporation of 2000 mm year^{-1}. The rainfall is temporally uneven, with approximately 80% occurring between June and September mainly as intensive storms. Heavy storms generate severe soil erosion, with an average annual sediment yield estimated to be ca. 200 t ha^{-1} year^{-1}. The elevation in the watershed ranges from 929 to 1075 m. A small check dam was built in 1974 downstream of the watershed (as shown in Fig. 1c), and remained well until now.

The main soil types are fine silt loess and Jurassic sandstone/mudstone (locally named Pisha sandstone). The hilly plateau surfaces are mostly covered by loose, fine loess, with relatively gentle slopes ($< 15°$), where sheet and rill erosions are widespread. The main crop is spring-sown maize in the terraced arable land in the relatively gentle slope area (Fig. 2). The weathered sandstone is mainly distributed in the steep slopes with gradients greater than 25°. These regions are mostly covered by very spare grass land or bare land (Fig. 2b).

Methods

In order to obtain the information about sedimentation behind the dam, three sedimentation profiles were extracted by digging pits (P1, P2, P3) upstream of the check dams in April 2015 (Fig. 1c). A representative sedimentation profile was obtained at site P1, and the other two sites (P2 and P3) were selected to check the flood couplet layers and to estimate sedimentation volume. The sedimentation in the dam was estimated to be approximately 11 m deep from the bottom to the current surface according to the dams' history and height of dam. However, the sediment pit at site P1 could only reach up to 3.0 m deep since water stored in the sediment leaked out from the bottom and sidewall of the profile. Afterwards, one side of the pit was carefully cleaned to expose the stratigraphy and the individual upward fining couplets. The profile was carefully documented to identify the individual flood couplets; a total of 24 couplets were

Fig. 1 Location of the study area, sampling sites, and soil types: **a** inlet map showing the location of the Huangfuchuan watershed, **b** map of the Huangfuchuan catchment showing the location of the Huangjiagou watershed, **c** sampling points in the watershed, **d** soil types in the watershed, **e** land use in the watershed
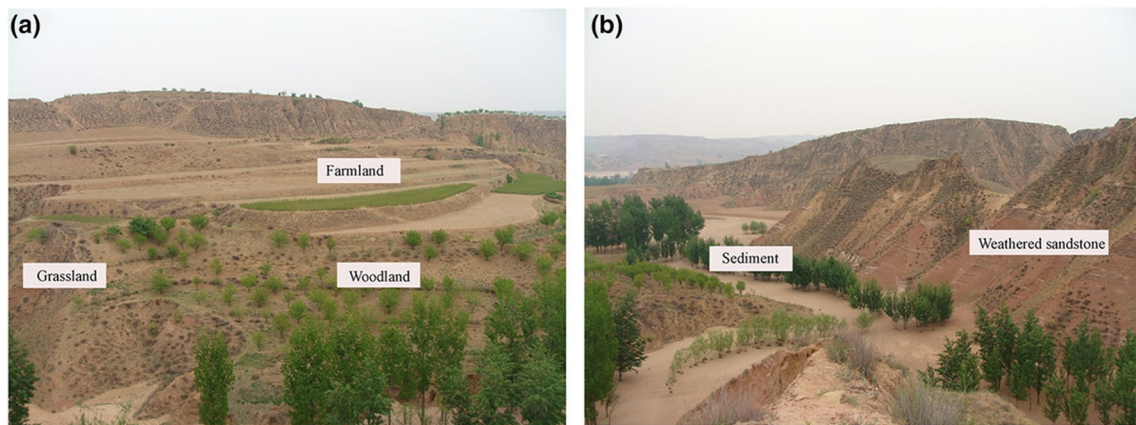
Fig. 2 Landscape of the Huangjiagou watershed

identified. According to the depth of the couplet, we divided each into three samples, and a few couplets were divided into two or four. A total of 39 sediment samples were collected from the profile.

In this study, all topsoil samples were collected from the upper 2 cm of the soils. Five topsoil subsamples (individual sample ≥ 500 g) were collected near each sampling point at a radius of 10 m and mixed into one composite sample. In total, 38 surface composite samples with 12 from uncultivated land (sparse grass), 13 from arable land, and 13 from bare sandstone were taken (Fig. 1c).

The width, length, and thickness of the sediment layers were measured in situ. A topography map (1:10,000) obtained from the Shaanxi Geodata Center was used to generate a digital elevation model (DEM). The topographic map was analyzed using the ArcGIS 10.2 software package (ESRI) to calculate the sediment volume. We did a topographic survey in the sedimentation area and adjacent slopes using the whole station to obtain the geometry and morphology of each flood couplet in the sedimentation. The volume of each flood couplet was then calculated by measuring the flood couplet depths and sedimentation area.

All soil source material and sediment samples were carried back to the laboratory, air-dried, disaggregated, and sieved to less than 2 mm prior to analysis of ^{137}Cs and ^{210}Pb. ^{137}Cs was measured at 661.6 keV, and the total ^{210}Pb activities of the samples was determined at 46.5 keV by gamma spectrometry using a hyperpure coaxial germanium detector coupled to a multi-channel digital analyzer system (ORTEC) with an analytical precision of approximately ± 6% at the 95% level of confidence.

We used a particle size analyzer (Malvern Mastersizer 2000) to measure the soil sample grain size. The low (X_{lf}) and high (X_{lf}) frequency magnetic susceptibility values were measured using a Bartington Instruments MS2B sensor (Bartington Instruments Ltd. 2000) to determine the frequency dependence of susceptibility (X_{fd}). The total organic carbon content was determined by wet oxidation with $K_2Cr_2O_7$ and H_2SO_4, and the total nitrogen (TN) content in the soil samples was assayed using the Kjeldahl method (Kalembasa and Jenkinson 1973). The δ^{13}C and δ^{15}N were analyzed in the Stable Isotope Laboratory of Hehai University, by using a PDZ Europa ANCA-GSL elemental analyzer interfaced to an isotope ratio mass spectrometer (Sercon Ltd., Cheshire, UK).

There were three main steps to quantify the contribution of the different potential sediment sources (Collins et al. 2010; Mukundan et al. 2010). Firstly, a mass conservation test was undertaken to remove the non-conservative tracers. Tracer selection should ensure that all sample concentrations of sinks fell within the observed range of source samples, and also that the sediment mix of each tracer was within the range of the mean concentration of the source soil (Wilkinson et al. 2013). Secondly, a two-stage statistical procedure was applied between sediment sources and sediment to identify the optimal set of fingerprinting properties. The ability of individual properties to discriminate sources was tested

by the nonparametric Kruskal–Wallis H test (Franz et al. 2014). A stepwise discriminant function analysis (DFA) was performed to further assess the discriminatory abilities of the tracer properties that passed the three constraints. DFA can identify a minimum optimal group of sediment tracers based on the minimization of Wilks' lambda. The results of the DFA were used to determine the proportion of samples that were accurately classified into the correct source groups (Walling 2005; Wilkinson et al. 2013).

A linear mixing model can be formulated on the basis of the chemical mass conservation as follows:

$$\sum_{i=1}^{n} P_s \times S_{si} = C_i \tag{1}$$

$$\sum_{i=1}^{n} P_s = 1 \text{ and } 0 \leq P_s \leq 1 \tag{2}$$

where P_s is the proportional percentage contribution from each sediment source category s; S_{si} is the mean concentration of the fingerprint property i in the source layer s; C_i is the concentration of the specific fingerprint property i in the sediment sample.

A multivariate mixing model was applied to these composite fingerprints to provide quantitative estimates of the relative contributions of each source (Collins et al. 2010; Lamba et al. 2015; Walling 2013; Zhao et al. 2017c). The model operates through minimizing the sum of the squares of the relative errors in the following function by changing the relative source proportions:

$$f = \sum_{i=1}^{n} \left\{ \left[C_i - \left(\sum_{s=1}^{m} P_s S_{si} Z_s \right) \right] \Big/ C_i \right\}^2 W_i \tag{3}$$

where n is the number of fingerprint properties comprising the optimum composite fingerprint; m denotes the number of sediment source categories; Z_s denotes the particle size correction factor for the source category; and W_i is the tracer discriminatory weighting. As proposed by Laceby et al. (2017), it is important to include the particle size correction factor in the model, particularly for the region where sediment sources have a wide range of particle sizes. The mixed model was subjected to two linear boundary conditions to ensure that the sum of contributions equals 1 and that the relative contributions (P_s) from the individual sediment sources were not negative. According to the soil types and land use/cover patterns, we categorized the sediment sources into three classes (arable land, uncultivated land, and bare sandstone).

The goodness of fit (GOF) was used to confirm that the mixing model generated meaningful sediment mixtures

(Collins et al. 2010). It represents the mean relative error between the actual fingerprint property concentrations in the sediment samples and the corresponding values predicted by the mixing model (Franz et al. 2014; Wilkinson et al. 2013).

$$\text{GOF} = 1 - \frac{1}{n} \times \sum_{i=1}^{n} \left\{ \left[C_i - \left(\sum_{s=1}^{m} P_s S_{si} \right) \right] \Big/ C_i \right\}^2 \quad (4)$$

Results

Sediment yield estimation from field samplings

The sediment volume of the check dam can be estimated on the basis of the storage capacity curve and sediment profile thickness. The total volume of sediment loss corresponding to the 3.0-m-deep profile was 1.51×10^5 m^3 in the Huangjiagou watershed. Based on the soil bulk density and sediment volume, a total of 2.05×10^5 t retained sediment was estimated during 2001–2014, which corresponded to an average annual sediment yield of 146.1 t ha^{-1} year^{-1}.

In order to estimate the sediment yield at event and annual scales, the flood couplets along the sedimentation profile have to be dated. Figure 3 shows the flood couplets characterized by fine sediment on the top and coarse sediment at the bottom. Through field surveys and careful inspection of the sediment profile, 24 flood couplets were identified, with the thinnest couplet of 1.5 cm and the thickest of 34.5 cm. To date the occurrence of each individual flood couplet, we compared the rainfall time series with the depth and volume of each flood couplet. Zhang et al. (2009) and Zhao et al. (2015) showed that higher rainfall amounts resulted in thicker flood couplets that contained more sediment. According to this principle, we found that the bottom couplet occurred in 2001. The top layer of the sediment had been mixed by cultivation effects, and corresponded to rainfall events from 2013 to 2014. As shown in Fig. 3, the five flood couplets that contained the greatest amount of sediment (> 10,000 t) corresponded to five rainfall events with daily rainfall higher than 80 mm. Among these couplets, four of them were thicker than 20 cm. They contributed approximately 36% of the total sediment yield, and each had a sediment yield of greater than 120 t ha^{-1}. Additionally, 2012 was an extremely wet year, and a total of 4.47×10^4 t sediment was retained by the check dam with annual sediment yield of 430 t ha^{-1} year^{-1}; whereas, 2011

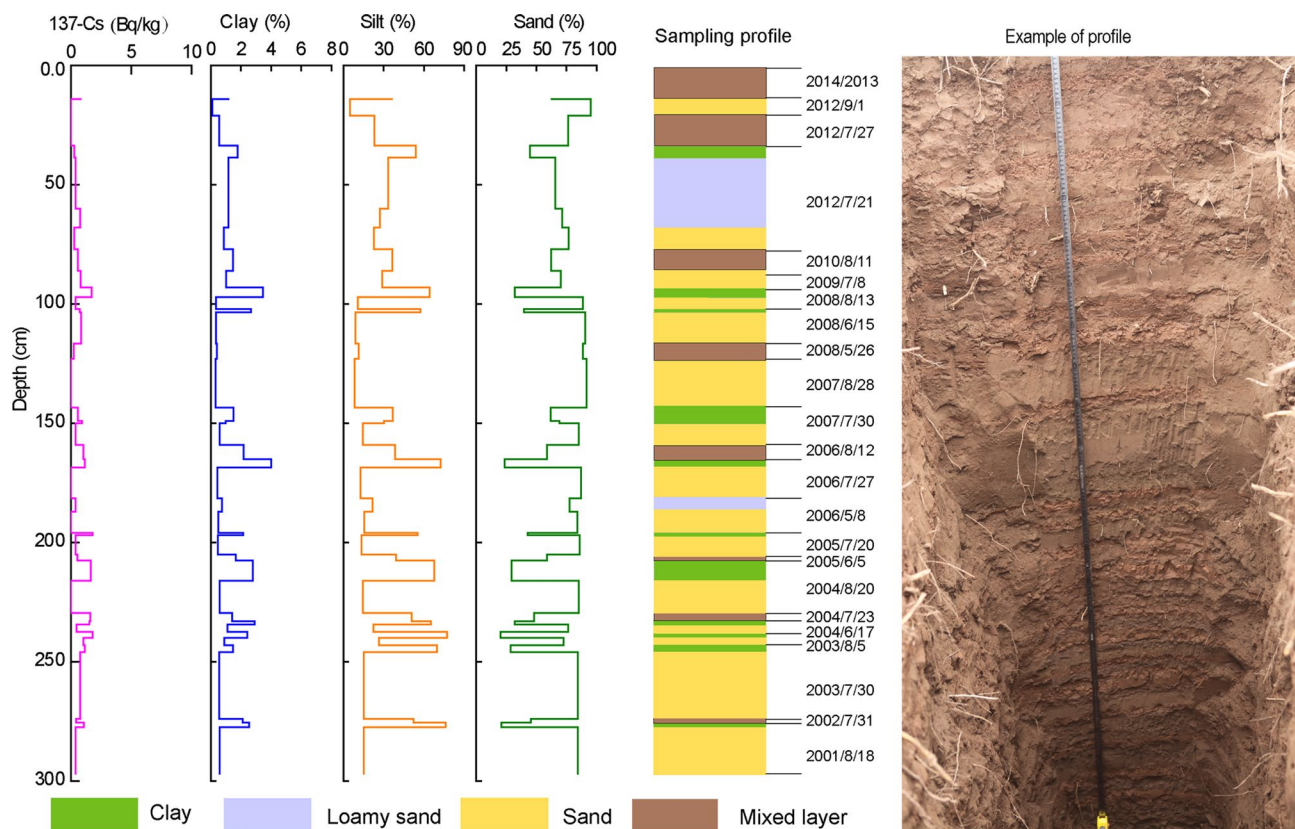**Fig. 3** Distributions of ^{137}Cs and soil particle size of the sedimentation profile in the Huangjiagou watershed

was an extremely dry year in which no flood event occurred, leading to no sediment yield.

Sediment source ascription

The Kruskal–Wallis *H* test was firstly applied to analyze the general characteristics of the soil properties. Table 1 displays the results of the test. Among all the physiochemical properties, X_{fd} was the weakest property that failed in the test, yielding a *p* value of 0.269. A number of fingerprints showed great potential for sediment source identification, given that the tests had *p* values lower than 0.005 (Table 1). However, following the recommendations of Koiter et al. (2013), TOC and grain size fractions were excluded from the analyses as they were considered as non-conservative properties. The multivariate DFA test suggested that three soil properties (X_{hf}, TN, and ^{137}Cs) comprised the optimum composite fingerprinting. Overall, the GOF for the sediment samples was estimated to be 86.8% in the watershed, which suggested that the mixed model gave an acceptable discrimination of the individual fingerprints in the sediment samples.

Figure 4 shows sediment sources from different land use/cover types at annual scale in the Huangjiagou watershed. We found that the sediment retained behind the check dams was mainly produced on steep gullies covered by weathered sandstone and the relatively gentle slopes by fine loess soil (Fig. 4). On average, approximately 74.06% of sediment originated from the weathered stone, followed by 15.67% from arable land, and the remaining 10.27% from uncultivated land. This suggested that sediment in the check dam mainly came from the weathered sandstone. Additionally, Fig. 4 shows that sediment sources from different land use/cover types varied greatly in each year. The sandstone contributed approximately 90% of sediment in 2012 and 56.1% in 2003. The contribution from arable land varied from 5.2% in 2005 to 44.6% within the period of 2013–2014.

Discussion

Temporal variation of sediment yield

Numerous studies reported that sediment load illustrated significant reduction in the Loess Plateau catchments during the past six decades, particularly after 2000 (Jiao et al. 2014; Yue et al. 2014). Similarly, the sediment load at Huangfu station in the watershed presented significant reductions. However, the annual sediment yield derived from sedimentation behind the check dam exhibited inconsistent changes with sediment load at Huangfu station (Fig. 5a). This may refer to the widespread check dams and reservoirs in the Huangfuchuan watershed. Tian et al. (2013) suggested that a total of 567 check dams and 16 reservoirs have been built until 2010 in the watershed, resulting in a large proportion of sediment trapped behind them. Annual sediment yield derived from the dam's deposits presented a general reference of sediment transported from hillslopes to river channels, whereas gauge observed sediment load was a fraction of sediment delivered by water flow that might be trapped by numerous soil and water conservation measures.
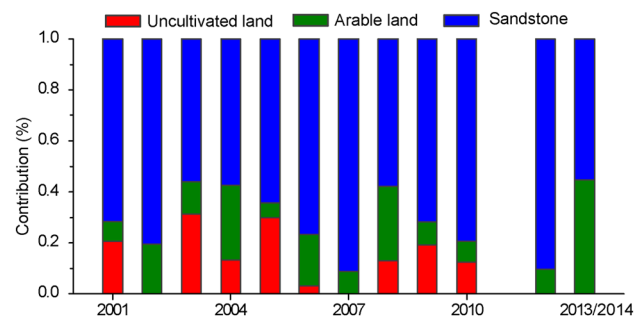

Fig. 4 Sediment sources apportionment at annual scales

Table 1 Kruskal–Wallis *H* test of the fingerprint properties in the Huangjiagou watershed

Soil properties	Uncultivated land		Arable land		Sandstone		*H*	*P*
	Mean	CV	Mean	CV	Mean	CV		
$\sigma^{13}C$ (‰)	−25.56	0.07	−25.52	0.05	−26.10	0.13	8.68	0.013*
$\sigma^{15}N$ (‰)	4.07	0.44	4.89	0.22	1.38	1.41	18.77	0.000*
TOC (g kg^{-1})	5.54	0.34	5.11	0.39	1.98	0.34	19.80	0.000*
TN (g kg^{-1})	0.51	0.19	0.63	0.11	0.26	0.24	27.77	0.000*
C/N	10.86	0.34	8.19	0.40	7.77	0.32	4.86	0.088
X_{lf} (10^{-8} m^3 kg^{-1})	36.57	0.19	38.55	0.09	13.36	0.41	25.42	0.000*
X_{hf} (10^{-8} m^3 kg^{-1})	34.33	0.18	36.38	0.09	12.70	0.42	25.38	0.000*
X_{fd} (%)	5.66	0.17	5.61	0.20	5.12	0.21	2.62	0.269
^{137}Cs (mBq g^{-1})	2.28	0.82	1.74	0.25	0.14	0.85	21.49	0.000*
^{210}Pb (mBq g^{-1})	44.52	0.34	40.63	0.24	21.44	0.60	16.20	0.000*

*$p \leq 0.05$

Fig. 5 Double mass curves between annual sediment yield and sediment load at Huangfu station (**a**), and annual rainfall (**b**)
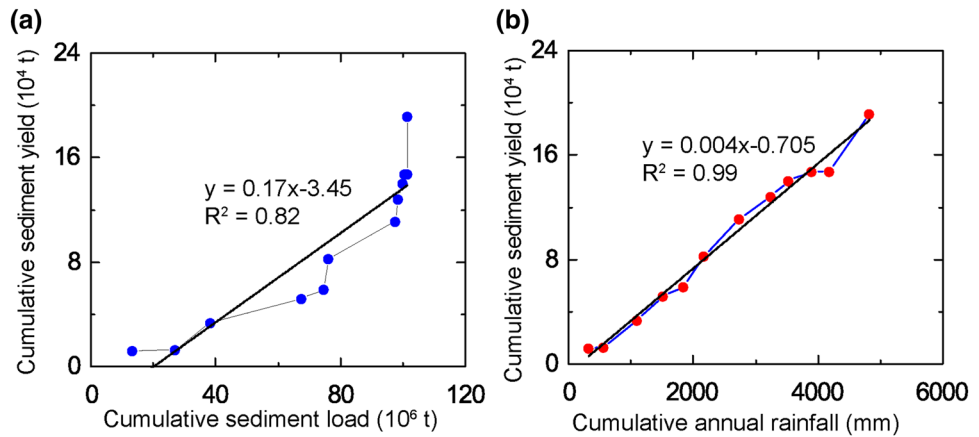
Figure 5b shows a relatively good linear relationship between the cumulative annual sediment yield and annual rainfall. However, it is different from Zhao et al. (2017c). They found that sediment yield was strongly related to land use changes and soil and water conservation measures. In contrast, the good linear relationship between cumulative sediment yield and cumulative annual rainfall indicated that sediment yield in our study area was largely related to the rainfall variation, rather than the changes in land use and land cover. This may be because the dominant sediment sources are mainly from bare sandstone, where no conservation measures were applied.

In the study area, an average annual sediment yield of 146.1 t ha^{-1} year^{-1} was estimated within the period of 2001–2014. In contrast, the specific sediment yield was higher than that of most regions on the Loess Plateau, which was attributed to relatively poor vegetation cover and bare weathered sandstone in the study area (Jiao et al. 2014). Furthermore, Wang and Jiao (1996) reported that heavy storms

occurred frequently in the Huangfuchuan watershed, and could bring large amounts of soil from steep poor land to the river, leading to extremely high sediment yield. Thus, further conservation measures are needed to reduce soil erosion in the steep sandstone region.

Results from comparable studies indicated that the specific sediment yield has shown decreasing trends since the 1950s in this region (Wei et al. 2017; Zhang et al. 2011; Zhao et al. 2015) (Table 2). However, the trend was not as significant as the observed sediment load at the Huangfu station. The specific sediment yields were above or close to 200 t ha^{-1} year^{-1} in the 1960s and 1980s, which were relatively higher than those during the later period in the Manhonggou and Mahaogou (Wei et al. 2017). This may largely result from the ecological restoration on the whole Loess Plateau. Vegetation cover has improved greatly since the implementation of the "Grain for Green" project. Our estimation showed much higher sediment yield than the values from Zhang et al. (2011). The inconsistencies

Table 2 Comparison of sediment yield through sedimentation behind the check dam close to the study area

Watersheds	Period	Area (km^2)	Sediment yield (t ha^{-1} year^{-1})	References
Xiaoshilata	1958–1972	0.64	171.9	
Yangjiagou	2007–2011	0.68	106.1	Zhao et al. (2017b)
Manhonggou	1985–1989	6.1	146.6	
	1990–1998		157.5	
	2000–2007		95.86	
Mahaogou	1985–1989	0.32	218.2	
	1990–1998		201.1	
	2000–2009		165.3	
Yuanzigou	2012–2014	1.52	101.2	
Dayanggou	2013–2014	0.69	94.19	Wei et al. (2017)
Xiheidaigou	1988–1992	3.2	242.2	
Wujiapo	1994–2003	1.1	83.33	
Baijiamen	2005–2009	0.48	27.11	Zhang et al. (2011)
Huangjiagou	2001–2014	1.04	146.1	This work

among these results may arise from the different land use and land cover in the watersheds. In addition, the spatial and temporal pattern of precipitation can strongly impact the sediment yields, leading to evident discrepancies among different watersheds.

Sediment source identification

The fingerprinting procedure provides information on the relative source contributions to the sediments deposited behind the check dam. The results indicated that the weathered sandstone contributed much more sediment than the uncultivated land and arable land (Fig. 6). This is consistent with the results obtained in the previous studies (Zhao et al. 2017b), which suggested that the specific sediment yield of the weathered sandstone was extremely high, and more than 60% of the net soil loss came from gully erosion. Consistently, Li et al. (1995) applied the [226]Ra values to identify the sediment sources and found that weathered sandstone contributed 55–76.5% of the total sediment in a small watershed.

It has to be noted that the use of the sedimentation-based approach for estimating the storage capacity of reservoirs or dams was sometimes questionable (Bussi et al. 2013; Foster and Walling 1994). Although it has been confirmed that this method was very useful to estimate the watershed sediment yield, de Vente et al. (2006) and Zhao et al. (2015) emphasized that some errors can occur in reservoir surveys, such as volume calculations and conversion from the sediment volume to mass. The sediment yields deduced from the deposits behind check dams are biased as a result of storage estimation and field survey.
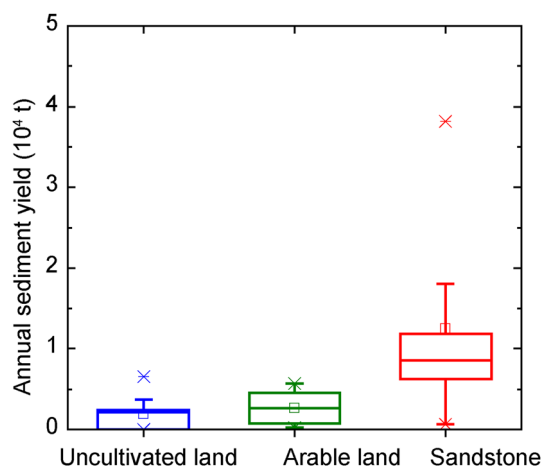
Sediment tracers with different sources

Different sediment properties were examined to obtain an optimum combination of fingerprints for sediment source apportionment. However, the results of the stepwise discriminant function analysis suggested that source sample properties were found to overlap (Table 3), which led to the discrimination analysis being unable to achieve 100% correct classification of source groups. This was particularly remarkable between arable land and uncultivated land. As shown in Fig. 7, the similar source sample properties between arable lands and uncultivated land can largely explain the difficulties in source apportionment. However, the analysis is not consistent with the results of Lasanta and Vicente-Serrano (2012) and Palazón et al. (2016), which demonstrated the influences of transition from arable land to natural forest.

Figure 7 exhibited six types of sample properties among the three sediment sources. It demonstrated the importance of the fallout radionuclide ^{137}Cs as a discriminator with largest differences between sediment sources. Large differences in total nitrogen in different land uses were related to the impacts of agricultural activities on the surface soils. Similarly, large differences in X_{hf} were detected between loess soil and weathered sandstone. The magnetic parameters of sediment may differ in important ways from those of the source material which were influenced by climate factors, soil types, and the components of magnetic minerals (Song et al. 2012). Although the particle size distribution of sandstone and loess soil showed evident differences, smaller differences were found in the particle size of arable land and uncultivated land (Fig. 7d).

In this study, we further tried to explore the potential of isotopes $\delta^{15}N$ and $\delta^{13}C$ for sediment source apportionment. For surface soils, which are related to the soil erosion processes, carbon and nitrogen are dominated by soil organic matter derived from decaying plants and vegetation. Fox and Papanicolaou (2008) reported that the success of these natural tracers was reflective of temporal and spatial soil erosion

Fig. 6 Sediment yield from different sources in the Huangjiagou watershed

Table 3 Stepwise discriminant function analysis of tracers

Steps	Tolerance	F to remove	Wilks' lambda
1			
X_{hf}	1.000	87.509	
2			
X_{hf}	0.854	11.580	0.183
TN	0.854	9.063	0.167
3			
X_{hf}	0.840	11.619	0.147
TN	0.694	11.034	0.144
[137]Cs	0.810	4.343	0.109
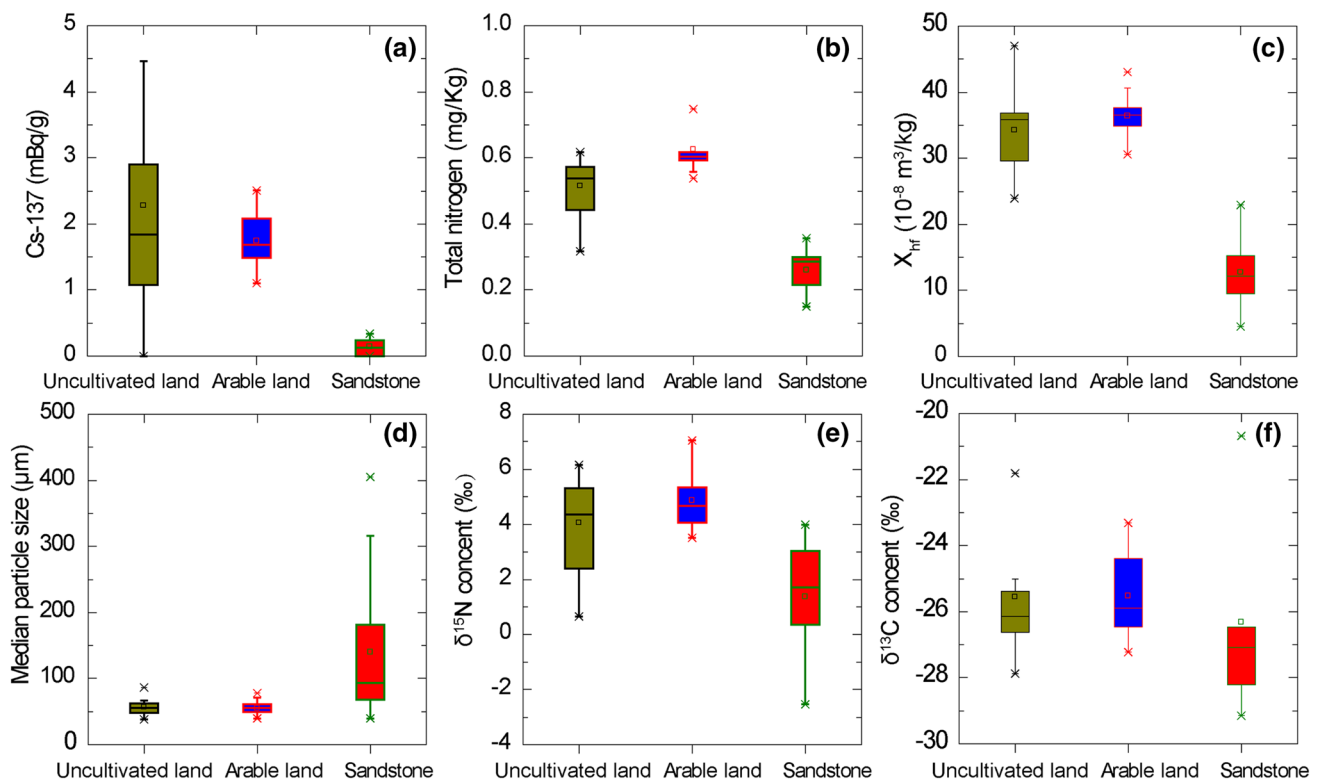
Fig. 7 Fingerprint properties from different sediment sources in the watershed. X_{hf} high frequency magnetic susceptibility

processes. The isotopes $\delta^{15}N$ and $\delta^{13}C$ of surface soil have been considered as indicators of different plant cover, land use, and land management (e.g., crop rotation, fertilization) at the sediment sources. As addressed by Davis and Fox (2009), tillage practice may break aggregates, expose labile organic matter, and generate a net shift in $\delta^{15}N$ and $\delta^{13}C$ due to the fractionation during mineralizations. The existing differences in isotopes were able to discriminate sediment sources from various land use types (i.e., uncultivated and arable land). Unfortunately, the DFA analysis test failure of these fingerprints for detection in the present study, suggesting specific soil features in the watershed. Soil tillage may have a relatively weak impact on the fine infertile loess soil in this region.

Conclusions

In this study, we estimated the sediment yield and sediment sources through a multivariate-based fingerprinting method in a dam-controlled watershed on the northern Loess Plateau. The main conclusions can be summarized as follows: The sampling profile exhibited evidence of 24 flood couplets corresponding to rainfall

events from 2001 to 2014. A total of 2.05×10^5 t sediment was trapped behind the check dam during the same period, with an average annual specific sediment yield of 146.1 t ha^{-1} year^{-1}. The sediment fingerprinting method suggested that the weathered sandstone was the most important sediment source, contributing approximately 74.06% of the total sediment, followed by 15.67% from arable land, and the remaining 10.27% from the uncultivated land in the Huangjiagou watershed. Results obtained from the fingerprinting method provided valuable information to investigate sediment sources in a dam-controlled watershed. It can improve our understanding of soil erosion processes to support sediment management at a watershed scale.

References

Bussi G, Rodriguez-Lloveras X, Frances F, Benito G, Sanchez-Moya Y, Sopena A (2013) Sediment yield model implementation based on check dam infill stratigraphy in a semiarid Mediterranean catchment. Hydrol Earth Syst Sci 17:3339–3354

Collins AL, Walling DE, Leeks GJL (1997) Sediment sources in the Upper Severn catchment: a fingerprinting approach. Hydrol Earth Syst Sci Dis 1:509–521

Collins AL, Zhang Y, Walling DE, Grenfell SE, Smith P (2010) Tracing sediment loss from eroding farm tracks using a geochemical fingerprinting procedure combining local and genetic algorithm optimisation. Sci Total Environ 408:5461–5471

Davis CM, Fox JF (2009) Sediment fingerprinting: review of the method and future improvements for allocating nonpoint source pollution. J Environ Eng 135:490–504

de Vente J, Poesen J, Bazzoffi P, Van Rompaey A, Verstraeten G (2006) Predicting catchment sediment yield in Mediterranean environments: the importance of sediment sources and connectivity in Italian drainage basins. Earth Surf Proc Land 31:1017–1034

Fleskens L, Stringer LC (2014) Land management and policy responses to mitigate desertification and land degradation. Land Degrad Dev 25:1–4

Foster IDL, Walling DE (1994) Using reservoir deposits to reconstruct changing sediment yields and sources in the catchment of the Old Mill Reservoir, South Devon, UK, over the past 50 years. Hydrolog Sci J 39:347–368

Fox JF, Papanicolaou AN (2007) The use of carbon and nitrogen isotopes to study watershed erosion processes. J Am Water Resour Ass 43:1047–1064

Fox JF, Papanicolaou AN (2008) Application of the spatial distribution of nitrogen stable isotopes for sediment tracing at the watershed scale. J Hydrol 358:46–55

Franz C, Makeschin F, Weiß H, Lorz C (2014) Sediments in urban river basins: identification of sediment sources within the Lago Paranoa catchment, Brasilia DF, Brazil – using the fingerprint approach. Sci Total Environ 466:513–523

Grauso S, Fattoruso G, Crocetti C, Montanari A (2008) Estimating the suspended sediment yield in a river network by means of geomorphic parameters and regression relationships. Hydrol Earth Syst Sci 12:177–191

Guzmán G, Quinton JN, Nearing MA, Mabit L, Gómez JA (2013) Sediment tracers in water erosion studies: current approaches and challenges. J Soils Sediments 13(4):816–833

Hessel R (2006) Consequences of hyperconcentrated flow for process-based soil erosion modelling on the Chinese Loess Plateau. Earth Surf Proc Land 31:1100–1114

Jiao JY, Wang ZJ, Zhao GJ, Wang WZ, Mu XM (2014) Changes in sediment discharge in a sediment-rich region of the Yellow River from 1955 to 2010: implications for further soil erosion control. J Arid Land https://doi.org/10.1007/s40333-40014-40006-40338

Jin Z, Cui BL, Song Y, Shi WY, Wang KB, Wang Y, Liang J (2012) How many check dams do we need to build on the Loess Plateau? Environ Sci Technol 46:8527–8528

Kalembasa SJ, Jenkinson DS (1973) A comparative study of titrimetric and gravimetric methods for the determination of organic carbon in soil. J Sci Food Agric 24:1085–1090

Koiter AJ, Owens PN, Petticrew EL, Lobb DA (2013) The behavioural characteristics of sediment properties and their implications for sediment fingerprinting as an approach for identifying sediment sources in river basins. Earth Sci Rev 125:24–42

Laceby JP, Olley J (2014) An examination of geochemical modelling approaches to tracing sediment sources incorporating distribution mixing and elemental correlations. Hydrol Process 29:1669–1685

Laceby JP, Evrard O, Smith HG, Blake WH, Olley JM, Minella JPG, Owens PN (2017) The challenges and opportunities of addressing particle size effects in sediment source fingerprinting: a review. Earth Sci Rev 169:85–103

Lamba J, Karthikeyan KG, Thompson AM (2015) Apportionment of suspended sediment sources in an agricultural watershed using sediment fingerprinting. Geoderma 239:25–33

Lasanta T, Vicente-Serrano SM (2012) Complex land cover change processes in semiarid Mediterranean regions: an approach using Landsat images in northeast Spain. Remote Sens Environ 124:1–14

Li SL, Su CJ, Bai LX, Wu LP, Xu JY (1995) Using ^{226}Ra to identify the sediment sources in a small watershed. Mt Res 13:199–202

Mekonnen M, Keesstra S, Baartman J, Ritsema C, Melesse A (2015) Evaluating sediment storage dams: structural off-site sediment trapping measures in Northwest Ethiopia. Cuadernos de Investigacion Geografica 41:7–22

Mukundan R, Radcliffe D, Ritchie J, Risse L, McKinley R (2010) Sediment fingerprinting to determine the source of suspended sediment in a southern Piedmont stream. J Environ Qual 39:1328–1337

Navas A, Lopez-Vicente M, Gaspar L, Palazon L, Quijano L (2014) Establishing a tracer-based sediment budget to preserve wetlands in Mediterranean mountain agroecosystems (NE Spain). Sci Total Environ 496:132–143

Palazón L, Latorre B, Gaspar L, Blake WH, Smith HG, Navas A (2016) Combining catchment modelling and sediment fingerprinting to assess sediment dynamics in a Spanish Pyrenean river system. Sci Total Environ 569:1136–1148

Pulley S, Rowntree K (2016) Stages in the life of a magnetic grain: sediment source discrimination, particle size effects and spatial variability in the South African Karoo. Geoderma 271:134–143

Romero-Díaz A, Alonso-Sarriá F, Martínez-Lloris M (2007) Erosion rates obtained from check-dam sedimentation (SE Spain). A multi-method comparison. Catena 71:172–178

Song Y, Hao QZ, Ge JY, Zhao DA, Zhang Y, Li Q, Zuo XX, Lu YW, Wang P (2012) Quantitative relationships between modern soil magnetic susceptibility and climatic variables of the Chinese Loess Plateau. Quat Sci 32:679–689 (in Chinese with English abstract)

Tian P, Zhao GJ, Mu XM, Wang F, Gao P, Mi ZJ (2013) Check dam identification using multisource data and their effects on streamflow and sediment load in a Chinese Loess Plateau catchment. J Appl Remote Sens 7(1):073697

Van Rompaey A, Krasa J, Dostal T (2007) Modelling the impact of land cover changes in the Czech Republic on sediment delivery. Land Use Policy 24 073697

Verstraeten G, Prosser IP (2008) Modelling the impact of land-use change and farm dam construction on hillslope sediment delivery to rivers at the regional scale. Geomorphology 98:199–212

Walling DE (2005) Tracing suspended sediment sources in catchments and river systems. Sci Total Environ 344:159–184

Walling DE (2013) The evolution of sediment source fingerprinting investigations in fluvial systems. J Soils Sediments 13:1658–1675

Walling DE, Collins AL, Stroud RW (2008) Tracing suspended sediment and particulate phosphorus sources in catchments. J Hydrol 350:274–289

Wang WZ, Jiao JY (1996) Rainfall and erosion sediment yeild in the Loess Plateau and sediment transportation in the Yellow River basin. Science Press, Beijing

Wei YH, He Z, Li YJ, Jiao JY, Zhao GJ, Mu XM (2017) Sediment yield deduction from check-dams deposition in the weathered sandstone watershed on the North Loess Plateau, China. Land Degrad Dev 28:217–231

Wilkinson SN, Hancock GJ, Bartley R, Hawdon AA, Keen RJ (2013) Using sediment tracing to assess processes and spatial patterns

of erosion in grazed rangelands, Burdekin River basin, Australia. Agric Ecosyst Environ 180:90–102

Xu XZ, Zhang HW, Zhang OY (2004) Development of check-dam systems in gullies on the Loess Plateau, China. Environ Sci Policy 7:79–86

Yue XL, Mu XM, Zhao GJ, Shao HB, Gao P (2014) Dynamic changes of sediment load in the middle reaches of the Yellow River basin, China and implications for eco-restoration. Ecol Eng 73:64–72

Zhang XC, Liu BL (2016) Using multiple composite fingerprints to quantify fine sediment source contributions: a new direction. Geoderma 268:108–118. https://doi.org/10.1016/j.geoderma.2016.01.031

Zhang XB, He XB, Wen AB, Walling DE, Feng MY, Zou X (2004) Sediment source identification by using ^{137}Cs and ^{210}Pb radionuclides in a small catchment of the Hilly Sichuan Basin, China. Chin Sci Bull 49:1953–1957

Zhang XB, Walling DE, He XB, Long Y (2009) Use of landslide-dammed lake deposits and pollen tracing techniques to investigate the erosional response of a small drainage basin in the Loess Plateau, China, to land use change during the late 16th century. Catena 79:205–213

Zhang YJ, Qin FC, Yue YJ (2011) Sediment deposits and organic carbon storage trapped behind the check dams in the Xiheidai watershed. Jiangsu Agric Sci 39:581–583

Zhang XC, Zhang GH, Liu BL, Liu B (2016) Using cesium-137 to quantify sediment source contribution and uncertainty in a small watershed. Catena 140:116–124

Zhang YQ, Long Y, Li B, Xu SJ, Wang XL, Liao J (2017) Use of reservoir deposits to reconstruct the recent changes in sediment yields from a small granite catchment in the Yimeng Mountain region, China. Geomorphology 293:167–177

Zhao GJ, Klik A, Mu XM, Wang F, Gao P, Sun WY (2015) Sediment yield estimation in a small watershed on the northern Loess Plateau, China. Geomorphology 241:343–352

Zhao G, Kondolf GM, Mu X, Han M, He Z, Rubin Z, Wang F, Gao P, Sun W (2017a) Sediment yield reduction associated with land use changes and check dams in a catchment of the Loess Plateau, China. Catena 148:126–137

Zhao GJ, Mu XM, Han MW, An ZF, Gao P, Sun WY, Xu WL (2017b) Sediment yield and sources in dam-controlled watersheds on the northern Loess Plateau. Catena 149:110–119

Zhao TY, Yang MY, Walling DE, Zhang FB, Zhang JQ (2017c) Using check dam deposits to investigate recent changes in sediment yield in the Loess Plateau, China. Glob Planet Change 152:88–98